Transient Behavior of Infiltrated Composites during Melt Layer Formation

MAURICE R. BERRY JR.,* MARTIN CRAWFORD,† AND FREDERICK B. GESSNER‡
Virginia Polytechnic Institute, Blacksburg, Va.

An analytical model is developed to demonstrate the effect of infiltrant melting on a porous-metal composite that retards its own heating rate by sacrificing its infiltrant when subjected to convective heating by a hot-gas stream. The transient, one-dimensional heat-transfer analysis is used to predict the surface temperature behavior of a composite with a melt layer on its exposed surface. The analysis accounts for both melt layer formation and depletion because of phase change and vaporization, respectively, but does not include hot-gas shearing effects. The governing equations were written in finite-difference form and programed for solution on a digital computer. Temperature distributions and interface locations have been computed for Ag, Cu, Sn, Pb, Mg, Li, and Zn infiltrants during the initial heating period before the melt layer begins to vaporize below the matrix surface. Inclusion of the melting process and of temperature-dependent properties in the analysis is shown to be necessary in order to describe adequately the early stages of the self-cooling process.

Nomenclature

A = intercept of vapor pressure-temperature curve, lbf/ft²
B = slope of vapor pressure-temperature curve, lbf-°R/ft²
c = specific heat, Btu/lbm-°R
h_o = convective heat-transfer coefficient with no vaporization effects, Btu/hr-ft²-°R
k = thermal conductivity, Btu/hr-ft-°R
L = depth of matrix, ft
m = nodal point at liquid-solid interface ($x = \delta_1$)
$\dot{m}_l,\dot{m}_v$ = mass rates of flow of liquid and vapor coolant, respectively, per unit surface area, lbm/hr-ft²
$\bar{m}_v$ = rate of formation of vapor, lbm/hr-ft²
n = nodal point at matrix surface ($x = L$)
ϕ = porosity of matrix: initial fraction of infiltrant volume in matrix relative to total volume
P_o = ambient pressure of hot-gas stream, lbf/ft²
P_v = vapor pressure of coolant, lbf/ft²
T = temperature, °R
T_c,T_m = critical and melting temperatures of coolant, °R
T_o = recovery temperature of hot-gas stream, °R
T_v = vaporization temperature of coolant, °R
T_{xi} = initial temperature distribution throughout composite, °R
v = nodal point at vapor-liquid interface ($x = \delta_2$)
x = distance normal to surface measured from insulated backface, ft
δ_1,δ_2 = distances from insulated back face to liquid-solid interface and vapor-liquid interface, respectively, ft
θ = time, hr; θ_1 = time at which temperature at original surface equals T_m; θ_2 = time at which surface temperature of liquid layer equals T_v at ambient pressure; θ_3 = time at which liquid layer starts to recede below original surface
λ_m,λ_v = latent heats of fusion and of vaporization of coolant, Btu/lbm
ρ = density, lbm/ft³

Subscripts

cl,cs = coolant in liquid phase and solid phase
m = matrix
ml,ms = weighted properties of matrix and liquid coolant composite, and of matrix and solid coolant composite
n = nodal point at matrix surface
nb = normal boiling condition of the coolant

Superscripts

$( )'$ = quantity after one additional time increment
$(\dot{})$ = time rate of change

Received March 6, 1969; revision received August 8, 1969. The present study was sponsored by NASA under Grant NGR-47-004-006 in conjunction with the NASA Multidisciplinary Grant Program at Virginia Polytechnic Institute. Much of the material presented in this paper formed part of a thesis submitted by M. Berry to Virginia Polytechnic Institute in partial fulfillment of requirements for the M.S. degree.

* Research Assistant, Department of Mechanical Engineering.
† Associate Professor of Mechanical Engineering; now Associate Professor of Engineering, University of Alabama in Birmingham, Birmingham, Ala.
‡ Assistant Professor of Mechanical Engineering; now Assistant Professor of Mechanical Engineering, University of Washington, Seattle, Wash.

Introduction

IN a previous study,[1] the transient behavior of an infiltrated porous tungsten composite was investigated from the standpoint of a one-dimensional, finite-thickness, flat-plate model with variable porosity and temperature-dependent properties.[2] However, the effect of melting of the infiltrant was neglected. Experimental data for infiltrated composites in rocket nozzles[3] have shown that a phase change causes expulsion of liquefied infiltrant onto the heated surface of the matrix. In arcjet studies, Ungar and Touryan[4] have observed the formation of a liquid layer on the heated surface of a copper-infiltrated tungsten matrix. For a period of time the surface was effectively insulated from the hot-gas flow because vaporization of a stable melt layer occurred at constant temperature. Resnick et al.[5] also observed molten pools on the surfaces of their test specimens during the early stages of the heating period, accompanied by a noticeable decline in the rate of temperature rise of the surface. The occurrence of stable liquid layers on the test specimens of Refs. 4 and 5 indicates that, for their test conditions, depletion of the liquid layer by hot-gas stream shearing effects was small in comparison to depletion by vaporization. Current models of transpiration and ablation cooling are inadequate to describe the self-cooling process because they are based on such limiting assumptions as steady or quasi-steady coolant flow. The present analysis is an extension of that presented in Ref. 1 and includes the effects of both melt layer formation and depletion due to melting and vaporiza-

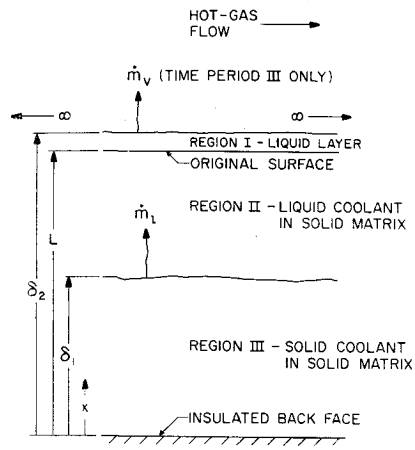

Fig. 1 Theoretical model, time periods II and III.

tion. Since shear is neglected, the analysis applies only for low shear conditions.

Theoretical Model

The composite is assumed to be an infinite slab of finite thickness. The general model considered is similar to that of Ref. 1. A porous matrix infiltrated with a coolant of a somewhat lower melting temperature, initially at a uniform temperature, is suddenly subjected to a strong convective heat input at the exposed surface. The other surface, or backface, is assumed to be thermally insulated. The overall heating process is divided into five time periods, similar to those suggested by Ungar and Touryan,[4] as follows:

I) The convective heating period prior to any phase change.

II) When the melting temperature of the coolant is attained at the exposed surface, the expansion of the melting coolant forces it onto the surface; the interface between solid and liquid coolant recedes through the matrix, sustaining the flow of liquid onto the surface.

III) The vaporization temperature is attained; initially this effect will tend to reduce the rate of buildup of the liquid layer. When the flow of vapor exceeds the flow of liquid onto the surface, the thickness of the layer will diminish. Figure 1 shows the model during periods II and III.

IV) The vapor-liquid interface recedes through the matrix; when it reaches the back face, all coolant is exhausted.

V) Heating continues in the matrix, until the melting temperature of the tungsten at the exposed surface is exceeded. It should be noted that the melting temperature of tungsten can be exceeded during period IV, before period V even begins.

Since the transient behavior during periods IV and V is analyzed in detail in Ref. 1, only periods I–III are considered herein. The major cooling mechanisms employed are the phase changes at the liquid-solid and vapor-liquid interfaces, convective cooling as the liquid coolant flows through the porous structure, and the insulating effect of the melt layer on the exposed surface. It is assumed that: a) thermal expansion is negligible except during a phase change; b) matrix and coolant temperatures are equal at any given depth in the porous matrix (as shown by Weinbaum and Wheeler[6] in their results of heat transfer in sweat-cooled metals); c) diffusion, chemical reaction, and shear between the coolant and hot-gas can be neglected; d) radiation from the hot gas to the heated surface is negligible compared to the convective heating.

Although it is recognized that hot-gas shearing effects in periods II and III may be very important, e.g., in rocket nozzle throats, inclusion of this loss mechanisn is not attempted in the present analysis because of the great complexity it would introduce. (The problem would become a transient, two-dimensional heat and mass transfer problem—cf. Eq. (5) of Ref. 4—whose numerical solution would be much more difficult than the already complex implicit-explicit-finite-difference solution of the transient, one-dimensional problem discussed herein. The liquid-solid infiltrant interface and the liquid layer-hot gas interface would become functions of both streamwise distance and time, cross flow of liquid infiltrant within the matrix would have to be taken into account, and all mass and energy balances would be complicated, making solution of the problem virtually intractable.)

In time period I ($0 \leq \theta \leq \theta_1$), we define an apparent thermal conductivity for the composite ($\phi \equiv$ porosity),

$$k_{ms} = k_m(1 - \phi) + k_{cs}\phi \tag{1}$$

A heat capacity per unit volume,

$$(\rho c)_{ms} = \rho_m c_m(1 - \phi) + \rho_{cs}c_{cs}\phi \tag{2}$$

is assigned locally to the composite. The energy balance of any internal element is

$$(\partial/\partial x)[k_{ms}\partial T/\partial x] = (\rho c)_{ms}\partial T/\partial\theta \tag{3}$$

The corresponding initial condition and boundary conditions are

$$\text{when } \theta = 0,\ T = T_{xi} \tag{4}$$

$$\text{at} \quad x = L, \quad k_{ms}\partial T/\partial x = h_o(T_o - T) \tag{5}$$

$$\text{at} \quad x = 0, \quad \partial T/\partial x = 0 \tag{6}$$

Solutions to Eq. (3) for the case of constant properties are charted in most heat-transfer texts (e.g., Ref. 7); they can be used only as an approximate check on the solution for our case.

In time period II ($\theta_1 < \theta \leq \theta_2$), the various regions that may exist are shown in Fig. 1. Whenever a liquid layer exists on the surface, there are three regions for which an energy balance must be written. For the liquid layer, region I ($L \leq x \leq \delta_2$),

$$\frac{\partial}{\partial x}\left[k_{cl}\frac{\partial T}{\partial x}\right] - \dot{m}_l\frac{\partial}{\partial x}[c_{cl}T] = \rho_{cl}c_{cl}\frac{\partial T}{\partial\theta} \tag{7}$$

where initially the temperature distribution is that determined from time period I at $\theta = \theta_1$, and the boundary conditions are

$$\text{at} \quad x = \delta_2, \quad k_{cl}\,\partial T/\partial x = h_o(T_o - T) \tag{8}$$

where $T < T_v(P_o)$

$$\text{at} \quad x = L, \quad k_{cl}\left.\frac{\partial T}{\partial x}\right|_{\text{I}} = k_{ml}\left.\frac{\partial T}{\partial x}\right|_{\text{II}} \tag{9}$$

where again an apparent conductivity of the matrix and liquid coolant is written as in Eq. (1). It is seen that the solution for this region is dependent on a temperature gradient in region II and the mass flow rate of liquid coolant. An energy balance at the melting interface ($x = \delta_1$) yields the following expression for the mass flow rate of liquid infiltrant per unit area[8]:

$$\dot{m}_l = \frac{\rho_{cs} - \rho_{cl}}{\rho_{cs}\lambda_m}\left[k_{ml}\left.\frac{\partial T}{\partial x}\right|_{\text{II}} - k_{ms}\left.\frac{\partial T}{\partial x}\right|_{\text{III}}\right] \tag{10}$$

Thus, the solution for region I is also dependent on a temperature gradient in region III, and, therefore, all regions must be solved simultaneously. The recession rate of the melting interface can be determined from a mass balance as

$$\dot{\delta}_1 = \dot{m}_l/[(\rho_{cl} - \rho_{cs})\phi] \tag{11}$$

subject to the conditions: $T = T_m$, at $x = \delta_1$, and $\delta_1 = L$ when $\theta = \theta_1$.

The growth rate of the liquid layer on the surface may also be determined from the mass flow rate of the liquid onto the surface[8]; i.e., $\dot{\delta}_2 = \dot{m}_l/\rho_{cl}$, subject to the initial condition that $\delta_2 = L$ when $\theta = \theta_1$.

In region II ($\delta_1 \leq x < L$), liquid coolant exists in a solid matrix, and the energy balance is

$$\frac{\partial}{\partial x}\left[k_{ml}\frac{\partial T}{\partial x}\right] - \dot{m}_l\frac{\partial}{\partial x}[c_{cl}T] = (\rho c)_{ml}\frac{\partial T}{\partial \theta} \qquad (12)$$

where initially the temperature distribution is that determined from time period I at $\theta = \theta_1$, and the boundary conditions are given by (9) and an alternative form of (10), namely, at $x = \delta_1$,

$$k_{ml}\left.\frac{\partial T}{\partial x}\right|_{II} - k_{ms}\left.\frac{\partial T}{\partial x}\right|_{III} = \frac{\dot{m}_l\rho_{cs}\lambda_m}{(\rho_{cs} - \rho_{cl})} \qquad (13)$$

In region III ($0 \leq x < \delta_1$), solid coolant exists within the matrix, so that the differential equation will be the same as that presented for period I. The initial condition is again the temperature distribution from time period I at $\theta = \theta_1$, and the boundary condition at $x = 0$ remains as in Eq. (6).

It should be noted that the existence of region III is dependent on the location of the liquid-solid interface δ_1. If $\delta_1 \leq 0$, region III does not exist and the boundary condition (13) for region II becomes $\partial T/\partial x = 0$ at $x = \delta_1 = 0$. Also, once δ_1 recedes to the backface of the matrix, the formation of liquid coolant ends.

In time period III ($\theta_2 < \theta \leq \theta_3$), the temperature of the liquid at the surface of the liquid layer exposed to hot-gas flow will continue to rise until T_v corresponding to the free-stream pressure is attained. An integrated form of the Clapeyron equation gives

$$T_v = B/(A - \log P_v) \qquad (14)$$

The heat associated with vaporization is absorbed at the surface of the layer. The effect of T_v on the latent heat of vaporization λ_v can be computed from[9]

$$\lambda_v = \lambda_{nb}[(T_c - T_v)/(T_c - T_{nb})]^{0.38} \qquad (15)$$

The rate of formation of vapor per unit area may be calculated from an energy balance at the surface of the liquid layer, and if it is assumed that all vapor formed leaves the surface,

$$\dot{m}_v = \bar{m}_v = \frac{1}{\lambda_v}\left[h_o(T_o - T_v) - k_{cl}\left.\frac{\partial T}{\partial x}\right|_I\right] \qquad (16)$$

When $\dot{m}_v$ surpasses $\dot{m}_l$, the thickness of the liquid layer will recede, and

$$\dot{\delta}_2 = (\dot{m}_l - \dot{m}_v)/\rho_{cl} \qquad (17)$$

The differential equations for δ_1 and the temperature distribution within the liquid layer and composite are the same as those developed for period II. The same boundary conditions also apply with the following exception:

$$\text{at} \quad x = \delta_2, \quad h_o(T_o - T_v) - k_{cl}\left.\frac{\partial T}{\partial x}\right|_I = \bar{m}_v\lambda_v \qquad (18)$$

The initial conditions for period III are that the temperature distribution and interface locations at $\theta = \theta_2$ are known from time period II. For both periods II and III, it is essential to note that although a liquid layer exists above the matrix surface, the underlying structure remains at $T < T_v(P_o)$.

Finite-Difference Analysis

The solution of the differential equation applicable to time period I for the case of temperature-dependent properties is not readily obtainable because of difficulties arising in the separation of variables technique of solution. At the instant melting occurs at the original surface, further difficulties arise in specifying the boundary conditions, because $\dot{m}_l$, $\dot{\delta}_1$, and the growth rate of the liquid layer above the surface are interdependent. Furthermore, the temperature distributions throughout the various regions at any instant of time are coupled at the interfaces and cannot be solved independently. Thus, a closed-form solution did not seem feasible. A finite-difference analysis was used to evaluate the time-dependent behavior of composite temperature, interface location, and coolant mass flow rate for various infiltrants. A computer program was written for this analysis.[8]

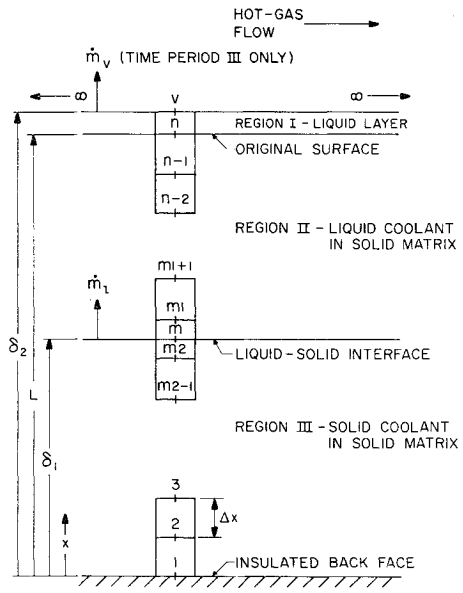

Fig. 2 Finite-difference model, time periods II and III.

The composite is divided into n-1 equal elements of height Δx and unit area, yielding n nodal points (Fig. 2). We consider first an explicit finite-difference equation for a general internal nodal point i that can be used for several regions during time periods I–III by selectively substituting the proper conditions at the time of application. This equation is used to evaluate the temperatures of the internal elements, excluding the boundary element at the heated surface and those elements adjacent to interfaces. The equation is not shown but is easily derived[8] by considering an energy balance on an element with a steady flow of coolant.

For explicit equations a "critical stability" must be satisfied to assure stability of the calculated temperature values. It is easily determined by reducing the time increment sufficiently for a given nodal spacing so that the coefficient of the unprimed temperature is positive. In general, it is governed by equations for nodal points other than the general internal points previously mentioned. To maximize permissible time and distance increments, implicit equations that require no stability criterion are used at nodal points adjacent to interfaces and at the heated surface.

In time period I, the temperatures of the internal nodal points are calculated from the general explicit equation by neglecting the flow of coolant and using apparent properties for the composite as discussed previously. An implicit equation can be developed for the nodal point at the heated surface. As a check on the implicit-explicit method of calculation, the results for time period I were duplicated using an entirely explicit scheme. For similar accuracy the calculation time more than doubled.

In time period II, the general explicit equation was used to calculate the temperatures of the interior nodal points 1 through $m2 - 1$ and $m1 + 1$ through $n - 1$. The remaining nodal points require a separate analysis due to the heat ab-

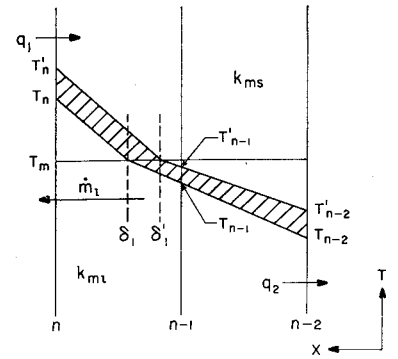

Fig. 3 Schematic of liquid-solid interface above nodal point n-1.

sorption accompanying melting at the liquid-solid interface and due to the liquid layer above the original surface. An implicit equation can be developed for nodal point n and a general interpolation equation can also be developed for the nodal points adjacent to the liquid-solid interface.[8]

To develop an implicit finite-difference equation for δ_1 when δ_1 lies between the original surface and nodal point $n-1$, let us consider Fig. 3. It is assumed that while δ_1 lies above $n-1$, the thickness of the liquid layer above the surface ($\delta_2 - L$) is sufficiently small so that we may let $T_v = T_n$. For this condition,

$$q_1 = h_o(T_o - T_n) = k_{ml}\frac{T_n - T_m}{L - \delta_1} \tag{19}$$

The shaded area of Fig. 3 represents the change of internal energy of the element ΔU and we may write

$$2\,\Delta U = (\rho c)_{ml}(T'_n - T_n)(L - \delta_1) + (\rho c)_{ml}(\delta_1 - \delta'_1) \times (T'_n - T_m) + (\rho c)_{ms}(T'_{n-2} - T_{n-2})[\delta_1 - (n-3)\Delta x] + (\rho c)_{ms}(\delta_1 - \delta'_1)(T_m - T'_{n-2}) \tag{20}$$

An energy balance on the element yields

$$(q_1 - q_2)\Delta\theta - \Delta U = \frac{\lambda_m \rho_{cs}}{(\rho_{cs} - \rho_{cl})}\dot{m}_l \Delta\theta \tag{21}$$

An implicit equation for the heat conducted out of the element q_2 may also be developed.[8] In finite-difference form the expression for the mass flow rate of the coolant is

$$\dot{m}_l = \phi(\rho_{cs} - \rho_{cl})(\delta_1 - \delta'_1)/\Delta\theta \tag{22}$$

and substitution of Eqs. (20) and (22) into the energy balance yields

$$A_3 - A_2 - (L - \delta'_1)[(\rho c)_{ml}(T'_n - T_m) + A_4] = 0 \tag{23}$$

where the A's are defined as

$$A_2 \equiv (\rho c)_{ms}(T'_{n-2} - T_{n-2})[\delta_1 - (n-3)\Delta x]$$

$$A_3 \equiv 2(q_1 - q_2)\Delta\theta + 2\rho_{cs}\lambda_m\phi(L - \delta_1) + (L - \delta_1)[(\rho c)_{ml}(T_n - T_m) + (\rho c)_{ms}(T_m - T'_{n-2})]$$

$$A_4 \equiv (\rho c)_{ms}(T_m - T'_{n-2}) + 2\rho_{cs}\lambda_m\phi$$

If the same assumption that led to Eq. (19) is applied to an energy balance at the exposed surface of the matrix, then

$$T'_n = \frac{k_{ml}T_m + h_o(L - \delta'_1)T_o}{k_{ml} + h_o(L - \delta'_1)} \tag{24}$$

Substitution of Eq. (24) reduces Eq. (23) to a quadratic equation in the unknown $(L - \delta'_1)$ from which the solution for δ'_1 can easily be found. Close inspection reveals that the positive sign must be used to insure $\delta'_1 < \delta_1$. This result enables one to calculate δ_1 and thus $\dot{m}_l$ from Eq. (22).

A similar approach can be used to develop a set of equations for predicting δ_1 implicitly when the interface has receded below nodal point $n-1$. The remaining unknowns in period II are the thickness of the liquid above the original surface ($\delta'_2 - L$) and its surface temperature T_v.

Consider a mass balance on the coolant above δ_1 at any time. If thermal expansion other than that due to phase change is neglected, then, on a unit area basis,

$$\rho_{cl}(T_m)(\delta'_2 - L) = [\rho_{cs}(T_m) - \rho_{cl}(T_m)]\phi(L - \delta'_1) \tag{25}$$

which can be written in alternative form to yield an implicit equation,

$$\delta'_2 - L = \phi(L - \delta'_1)[\rho_{cs}(T_m)/\rho_{cl}(T_m) - 1] \tag{26}$$

To develop an expression for T'_v, the heat storage in the liquid layer can be neglected, since the maximum thickness of this layer is at most 5.0% of the total composite thickness for coolants and porosities considered in the present work. With this assumption, an energy balance at the exposed surface of the liquid layer yields

$$T'_v = \frac{h_o T_o(\delta'_2 - L) + k_{cl}T_n}{h_o(\delta'_2 - L) + k_{cl}} \tag{27}$$

Calculations proceed until T'_v is equal to the vaporization temperature of the coolant, which concludes time period II.

In time period III, the determination of all temperatures, the location of δ_1, and $\dot{m}_l$ below the original surface are obtained from the same equations discussed in period II, but we must also account for vaporization at the exposed surface. An implicit equation for the temperature of the original heated surface can be developed by assuming negligible heat storage in the liquid layer and realizing that the exposed surface of the liquid layer remains at T_v. A mass balance and an energy balance over an increment of time must be solved simultaneously to determine $\dot{m}_v$ and $\dot{\delta}_2$.[8] When $\delta_2 = L$, period III is concluded.

Results and Discussion

An extensive search was conducted to determine the thermo-physical properties of silver, magnesium, copper, tin, lithium, zinc, and lead. In general, the k's and c's of these coolants, as well as for the tungsten matrix, are strong functions of temperature over the anticipated temperature range. Conveniently, straight lines approximate much of the data to within the variations reported in different references. For those properties where the second-order term is necessary, least-squares fits were performed.[8] In some instances, the properties of the coolants in liquid phase were not obtained, in which case the property was assumed constant and equal to the value obtained for the liquid coolant at its normal melting point.

The infiltrants were evaluated for a flame temperature and throat pressure typical of a high-energy solid-propellant rocket motor.§ The general conditions specified for all cases are as follows: $T_o = 6660°\text{R}$, $P_o = 226$ psia, $h_o = 1303$ Btu/hr-ft²-°R, $L = 2.0$ in., and $T_{xi} = 530°\text{R}$. These conditions are the same as those specified in Refs. 1 and 10. It was anticipated that the results could be compared so that the effects of temperature-dependent properties and of the melting process could be shown. The specific heat of the tungsten matrix reported in Ref. 1, however, is approximately 18% higher than the average value used in the present work, and, therefore, a direct comparison is not possible. Computer results of the present study do show, however, that the difference in specific heats can account for as much as a 5% variation in the temperature of the original surface at any time if other property values are assumed to be the same in both studies.

Results are given in Figs. 4–6 for $\phi = 0.2$. The curves terminate at that time when the coolant begins to vaporize within the matrix ($\theta = \theta_3$) unless otherwise indicated. The

§ Again, the reader is cautioned that shear effects are neglected.

temperature response of the original surface for solid tungsten was obtained as a baseline of comparison by letting $\phi = 0$. Calculations were also made for solid tungsten using thermal properties given in Ref. 1. A comparison with results reported in Ref. 1 showed excellent agreement throughout the entire heating period. Figure 4 shows that matrices infiltrated with lead and tin result in early surface temperatures somewhat higher than that of solid tungsten (so does Li, not shown). However, the rate of surface temperature rise may be greatly retarded by the vaporization of these coolants within the matrix during later time periods.[1,2] The δ_1's for all seven infiltrants are shown in Fig. 5, and the growth and depletion of the liquid layers for silver, tin, copper, and lead are compared in Fig. 6. That portion of each distribution in Fig. 6 with negative slope corresponds to time period III when the melt layer on the exposed surface vaporizes. The apparent discontinuities in slope at certain points are explainable by remembering that evaporation of the melt layer at temperatures below $T_v(P_o)$ was neglected. Inclusion of this minor cooling mechanism in the analysis would have had the effect of smoothing the apparent slope discontinuities.

The total time for recession of the silver vapor-liquid interface to the original surface is 48.6 sec (Fig. 6). This behavior is attributable to the relatively high boiling point of silver at the local pressure (5705°R). In reference to Fig. 4 for the silver infiltrant, the temperature of the heated surface is lower than that of a solid tungsten slab because of the increased thermal diffusivity of the composite with silver as an infiltrant. This effect diminishes with time, so that the silver curve approaches the solid tungsten curve as the boiling point of silver is approached at the exposed surface of the liquid layer. The importance of the liquid layer is indicated by the relatively flat portion of the surface temperature response curve, which corresponds to time period III. Even though the maximum possible thickness of the liquid layer was realized (about 1.0% of the total composite thickness), the temperature difference across the liquid layer was small compared to that for other coolants because of the high conductivity of silver. This factor, as well as the relatively high latent heat of vaporization of silver, accounts for the essentially constant temperature at the original surface when a liquid layer is present.

For copper $T_v(P_o)$ is higher than the melting temperature of the tungsten matrix. Consequently, the original surface

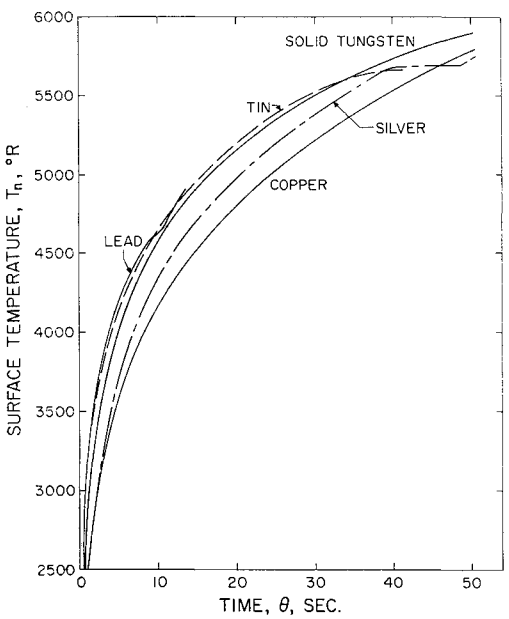

Fig. 4 Surface temperature response for lead, tin, copper, and silver infiltrants ($\phi = 0.2$).

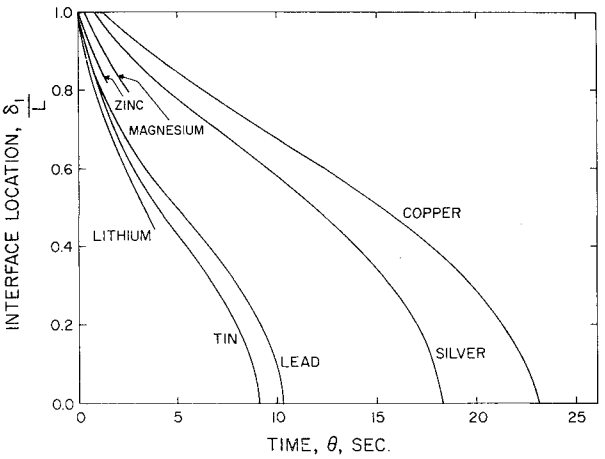

Fig. 5 Liquid-solid interface recession for various coolants ($\phi = 0.2$).

of the matrix begins to melt while a liquid layer exists on its surface. The advantage of infiltrating with copper is therefore limited.

The behavior of tin is similar to that of silver, since their boiling points are about the same, but tin's lower melting point (1081°R) causes liquid-solid interface recession to occur much sooner (Fig. 5), and its smaller volume change on fusion leads to a thinner liquid layer (Fig. 6). The portion of the surface-temperature response curve that corresponds to time period III is not as flat as that of silver because of the low conductivity of tin (Fig. 4). The relatively poor thermal diffusivity of the composite also causes the surface to run hotter than the tungsten slab during early heat-up stages (Fig. 4).

Lead possesses the same general characteristics as tin. Because of its lower boiling point (4875°R) vaporization below the original surface occurs sooner (13.3 vs 40.7 sec, Fig. 6). Complete liquid-solid interface recession occurs shortly after vaporization begins at the exposed surface. This behavior results in an initial decrease in the rate of surface temperature rise (Fig. 4) followed by immediate increase when the flow of liquid onto the surface ceases. Since Zn, Mg, and Li (not shown in Fig. 6) have relatively low boiling points, their computed normalized liquid layer thicknesses show sharp peaks of 0.20%, 0.15%, and 0.16% at 1.2, 2.2, and 3.3 sec, respectively (before liquid-solid interface recession is com-

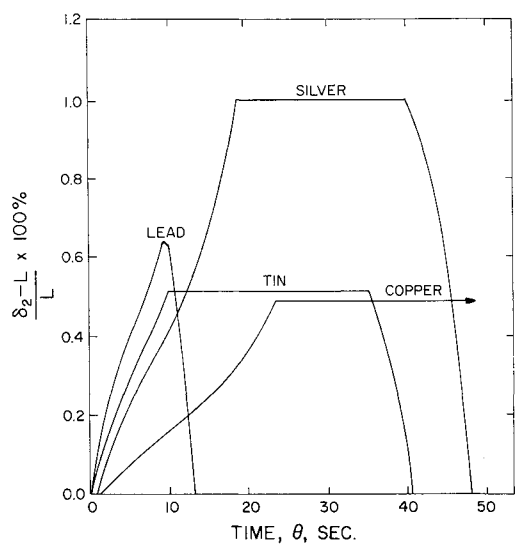

Fig. 6 Growth and depletion of melt layer for lead, tin, copper, and silver infiltrants ($\phi = 0.2$).

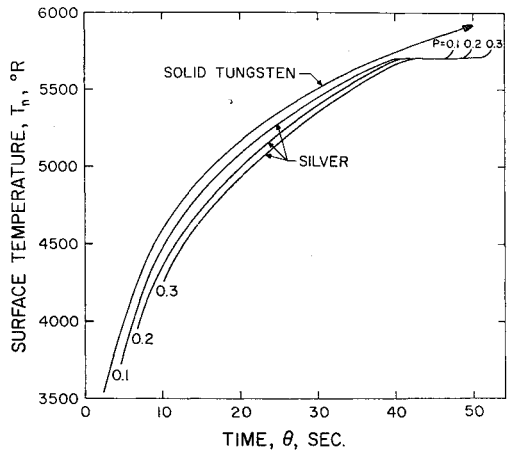

Fig. 7 Effect of porosity on surface temperature response for silver infiltrant (ϕ = 0.1, 0.2, and 0.3).

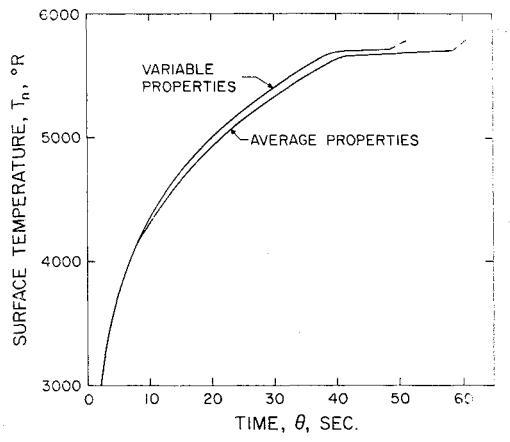

Fig. 8 Effect of property values on surface temperature response for silver infiltrant (ϕ = 0.2).

pleted; see Fig. 5), and vaporization beneath the surface begins ~0.3 sec later for each.

Figure 7 shows that with silver, a considerable increase in conduction cooling occurs with an increase in porosity during the early stages of the heating period because of the high conductivity of silver compared to that of the tungsten matrix. The tendency for conduction cooling effects to diminish as the boiling temperature of the coolant is approached is apparent. An interesting result is that recession of the liquid-solid interface for each silver case ceased at essentially the same time (18 sec). This behavior is thought to be due to increased conductivity of the composite with an increase in silver content. The major advantage of increasing porosity is seen to be in the increased length of the flat portion of the temperature response curve. This does not indicate, however, that longer heating times may be obtained by increasing the porosity. Gessner et al.[1] report that the surface temperature response curves for a silver infiltrant and porosities of 0.2 and 0.8 converge as vapor-liquid interface recession proceeds below the heated surface. It is suggested in Ref. 1 that a graded matrix with highest porosity at the exposed surface is more efficient in increasing allowable heating time. In any case, a compromise between porosity, mechanical strength, and manufacturing limitations must be made.

Finally, Fig. 8 shows the effect of using constant average property values for each particular phase, rather than temperature-dependent properties. The computed surface temperatures based on average properties are somewhat lower. The increase of the flat portion of the surface-temperature response curve when average properties are used is misleading. The amount of liquid which expands onto the heated matrix surface is directly related to the density difference $\rho_s - \rho_l$ at the melting point. This difference is normally 2 to 7% of the solid density when based on local temperature. When average density values for each phase are used, $\rho_s - \rho_l$ becomes nearly 13%, which increases the maximum melt-layer thickness by more than twofold and, in turn, leads to an overestimation of inhibition of surface temperature rise because of melt-layer vaporization.

Conclusions and Recommendations

A coolant with large volume change on fusion, high thermal diffusivity, and high latent heat of vaporization is desirable for maximum efficiency of infiltrated composites. The effect of the melting process on the temperature response of an infiltrated composite can be important, in that in some cases, the temperature of the heated surface remains essentially constant while vaporization of the melt layer occurs. The need to include accurate temperature-dependent thermal properties in the analysis was demonstrated. Future analytical work should attempt to account for hot-gas stream shearing effects on depletion of the liquid layer.

References

[1] Gessner, F. B., Ingram, R. J., and Seader, J. D., "Summary Report, Self-Cooled Rocket Nozzles," RTD-TDR-63-4046, Vol. 2, (AD-601574), March 1964, Wright-Patterson Air Force Base, Ohio.

[2] Seader, J. D., Rivers, W. J., and Ingram, R. J., "Effect of Porosity Zoning and Matrix Material on the Performance of Self-Cooled Nozzle Throat Inserts," *Journal of Spacecraft and Rockets*, Vol. 3, No. 7, July 1966, pp. 1138–1140.

[3] Schwarzkopf, P. and Weisert, E. D., "Summary Report, Self-Cooled Rocket Nozzles," RFD-TDR-63-4046, Vol. 3, (AD-473691), Aug. 1965, Wright-Patterson Air Force Base, Ohio.

[4] Ungar, E. W. and Touryan, K. J., "Ablation Mechanism for Impregnated Tungsten," *AIAA Journal*, Vol. 3, No. 10, Oct. 1965, pp. 1949–1950.

[5] Resnick, R. et al., "Cooling of Porous Tungsten Structures by Evaporation of Infiltrated Material," *Metals Engineering Quarterly*, Vol. 3, No. 2, May 1963, pp. 51–59.

[6] Weinbaum, S. and Wheeler, H. L., Jr., "Heat Transfer in Sweat-Cooled Metals," *Journal of Applied Physics*, Vol. 20, No. 1, Jan. 1949, pp. 113–122.

[7] Schneider, P. J., "Transient Systems. Heating Cooling," *Conduction Heat Transfer*, 2nd ed., Addison-Wesley, Reading, Mass., 1957, pp. 229–271.

[8] Berry, M. R., Jr., Crawford, M., and Gessner, F. B., "An Analysis of the Transient Behavior of Infiltrated Tungsten Composites Including the Effect of the Melt Layer," Final Technical Report, NASA Grant NGR-47-004-006, Project 31655, April 1968, Virginia Polytechnic Institute, Blacksburg, Va.

[9] Watson, K. M., "Thermodynamics of the Liquid State, Generalized Prediction of Properties," *Industrial and Engineering Chemistry*, Vol. 35, No. 4, 1943, pp. 398–406.

[10] Gessner, F. B. et al., "Analysis of Self-Cooling with Infiltrated Porous Tungsten Composites," *Journal of Spacecraft and Rockets*, Vol. 1, No. 6, Nov.-Dec. 1964, pp. 643–648.